Detecting dark matter oscillations with gravitational waveforms

P. Valageas

IPhT - CEA Saclay

Collaboration with Ph. Brax, C. Burrage, J. Cembranos

Marseille - October 15, 2024
GdR GW

arXiv: 2402.04819

I- Ultra-light Dark Matter as a Dark Matter candidate

A) Known properties of DM

- 27% of the energy density of the universe
- Cold (non-relativistic)
- Dark: small electromagnetic interactions
- Collisionless / pressureless: small self-interactions or interactions with baryons

Energy content of the Universe

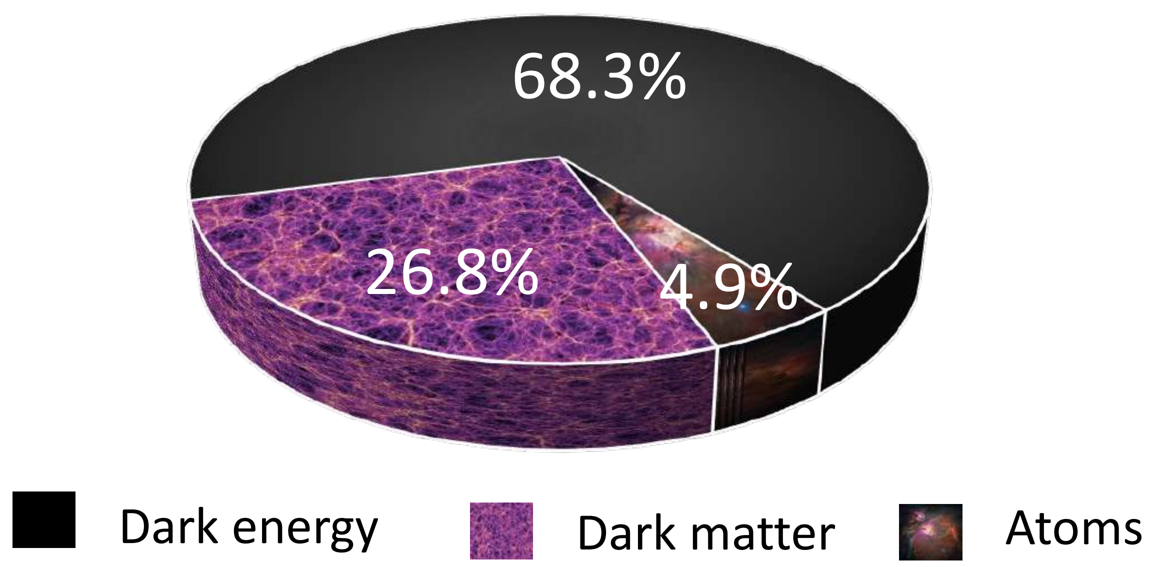

However there remains a huge uncertainty on its mass and many scenarios exist, from elementary particles to macroscopic objects:

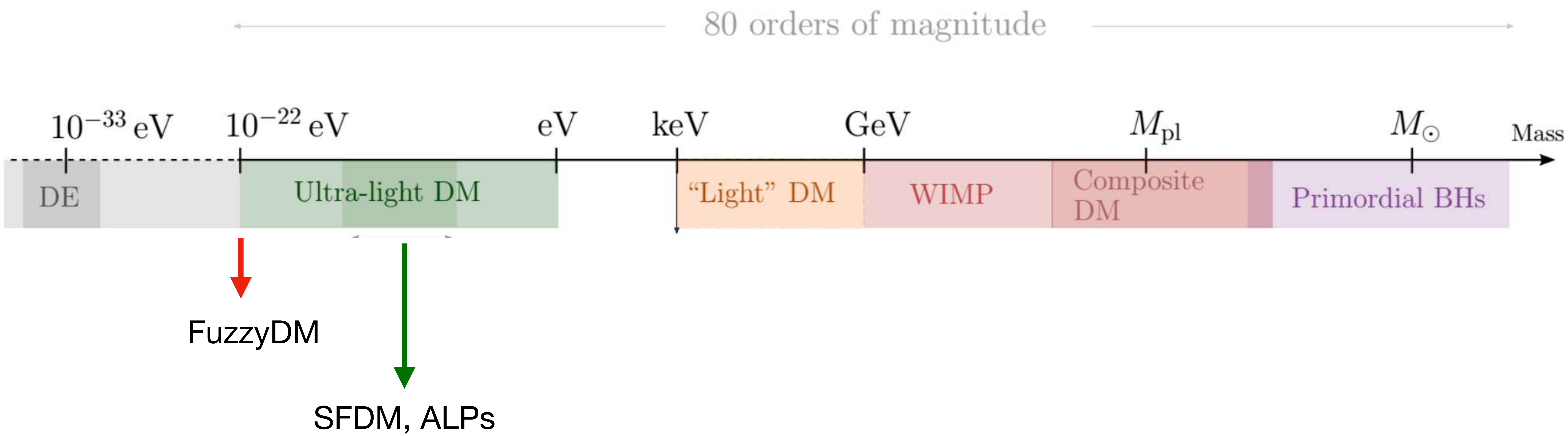

B) Many DM candidates

Bertone and Tait, 1810.01668

C) Ultra-light dark matter $10^{-22}\,\mathrm{eV} < m < 1\,\mathrm{eV}$

Renewed interest in recent years (Hui, Ostriker, Tremaine, Witten 2017), especially since WIMPs have not been detected yet and ULDM might alleviate some small-scale tensions of LCDM.

Missing satellite problem

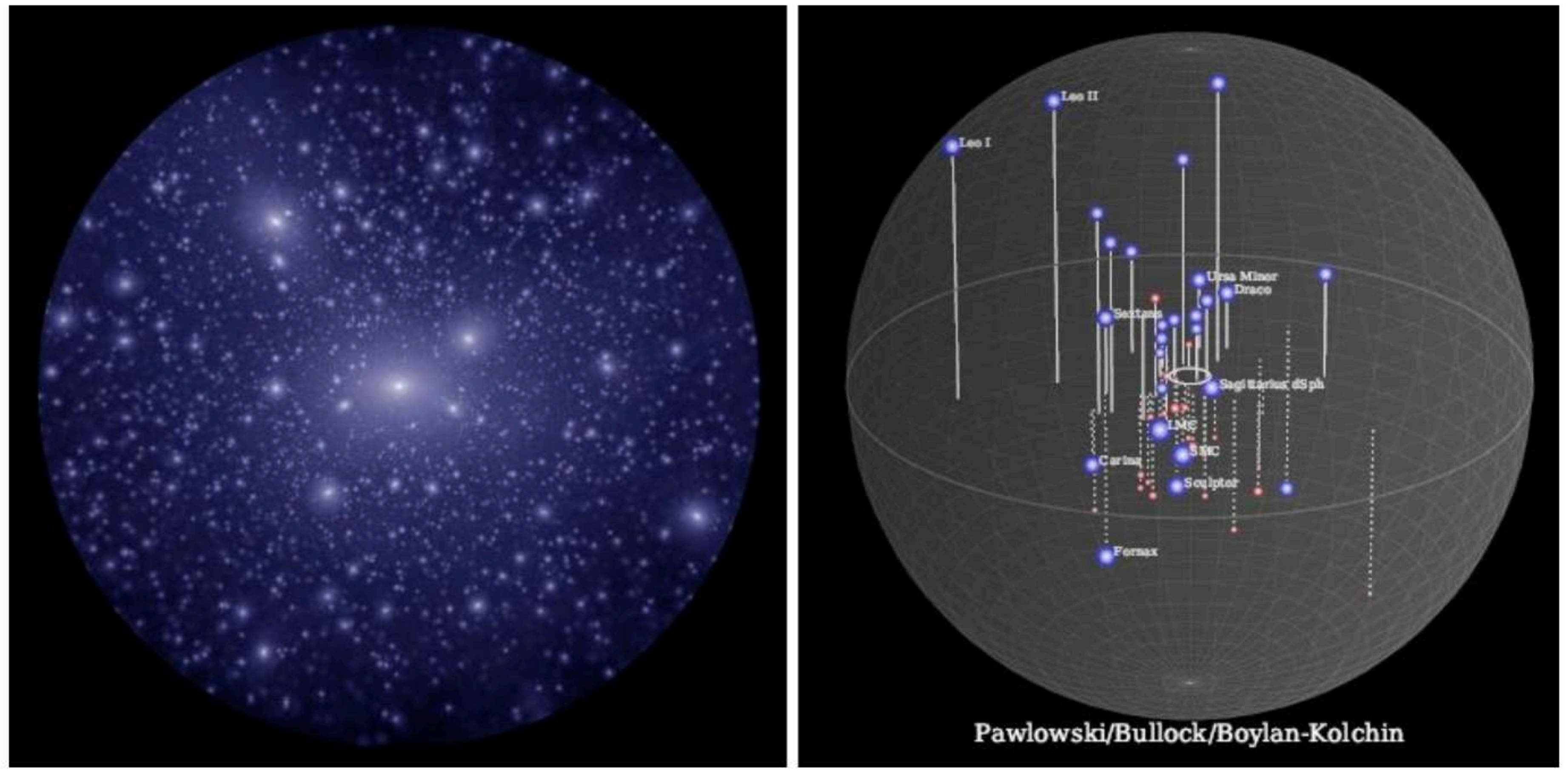

Predicted ΛCDM substructure

Simulation by V. Robles and T. Kelley and collaborators.

Known Milky Way satellites

James S. Bullock, M. Boylan-Kolchin, M. Pawlowski

Core/cusp problem

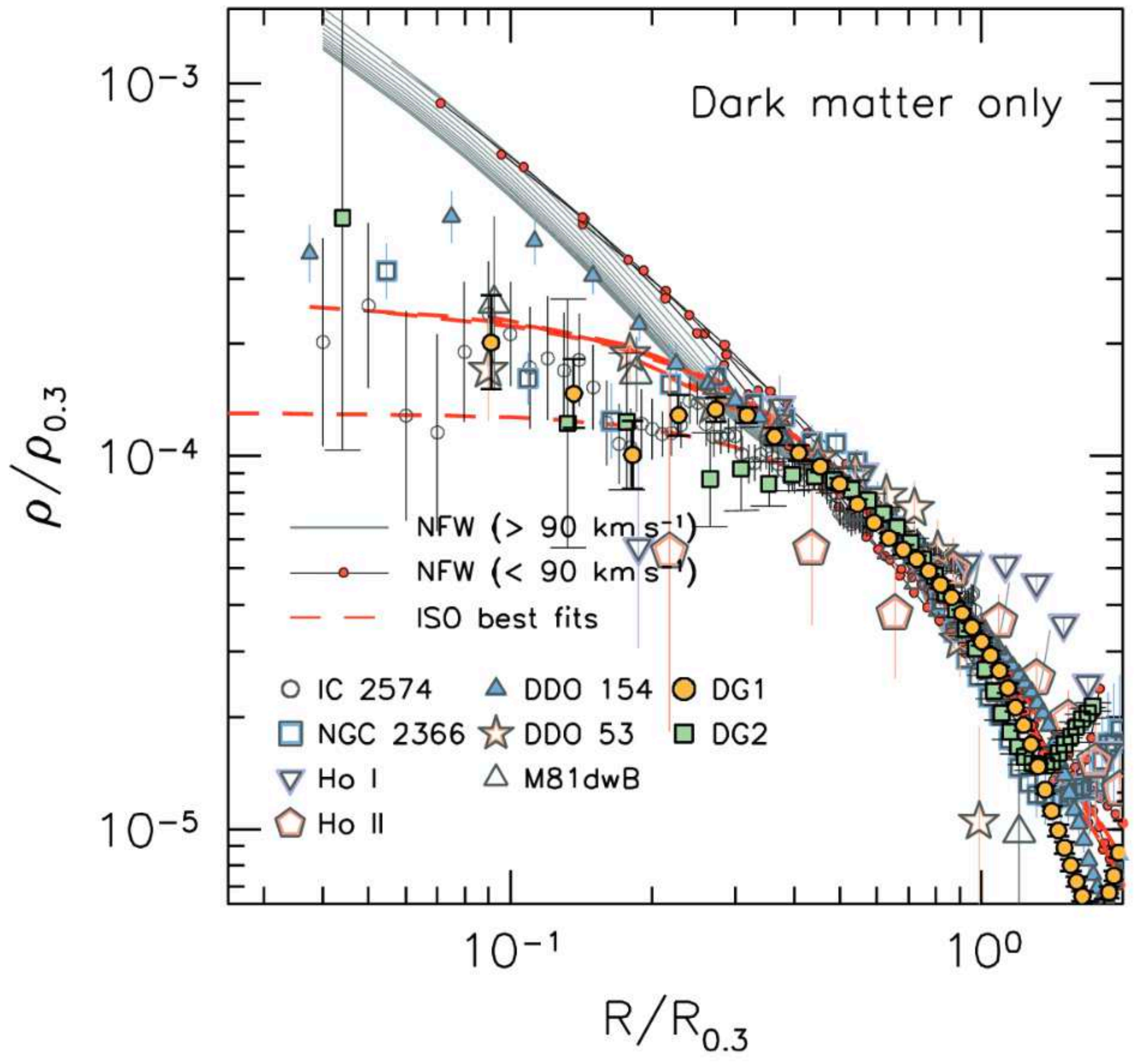

Density profiles observations and simulations

Antonino Popolo, Morgan Le Delliou (2017)

These problems may be solved by a proper account of baryonic physics (feedback from Supernovae and AGN), but ULDM remains an interesting candidate on its own.

D) Fuzzy dark matter $m \sim 10^{-22}\mathrm{eV}$

De Broglie wavelength: $\boxed{\lambda_{\mathrm{dB}} = 2\pi/(mv) \simeq \left(\frac{m}{10^{-22}\,\mathrm{eV}}\right)^{-1} \left(\frac{v}{100\,\mathrm{km/s}}\right)^{-1} \mathrm{kpc}}$

The DM density field behaves like CDM on large scales but structures are suppressed below λ_{dB}

In particular, hydrostatic flat cores (« solitons ») can form at the center of DM halos.

For Fuzzy Dark Matter: $m \sim 10^{-22}\mathrm{eV}$ $\lambda_{\mathrm{dB}} \sim 1\,\mathrm{kpc}$

However, this model already seems ruled out by Lyman-alpha forest power spectra (because of this suppression of small-scale power).

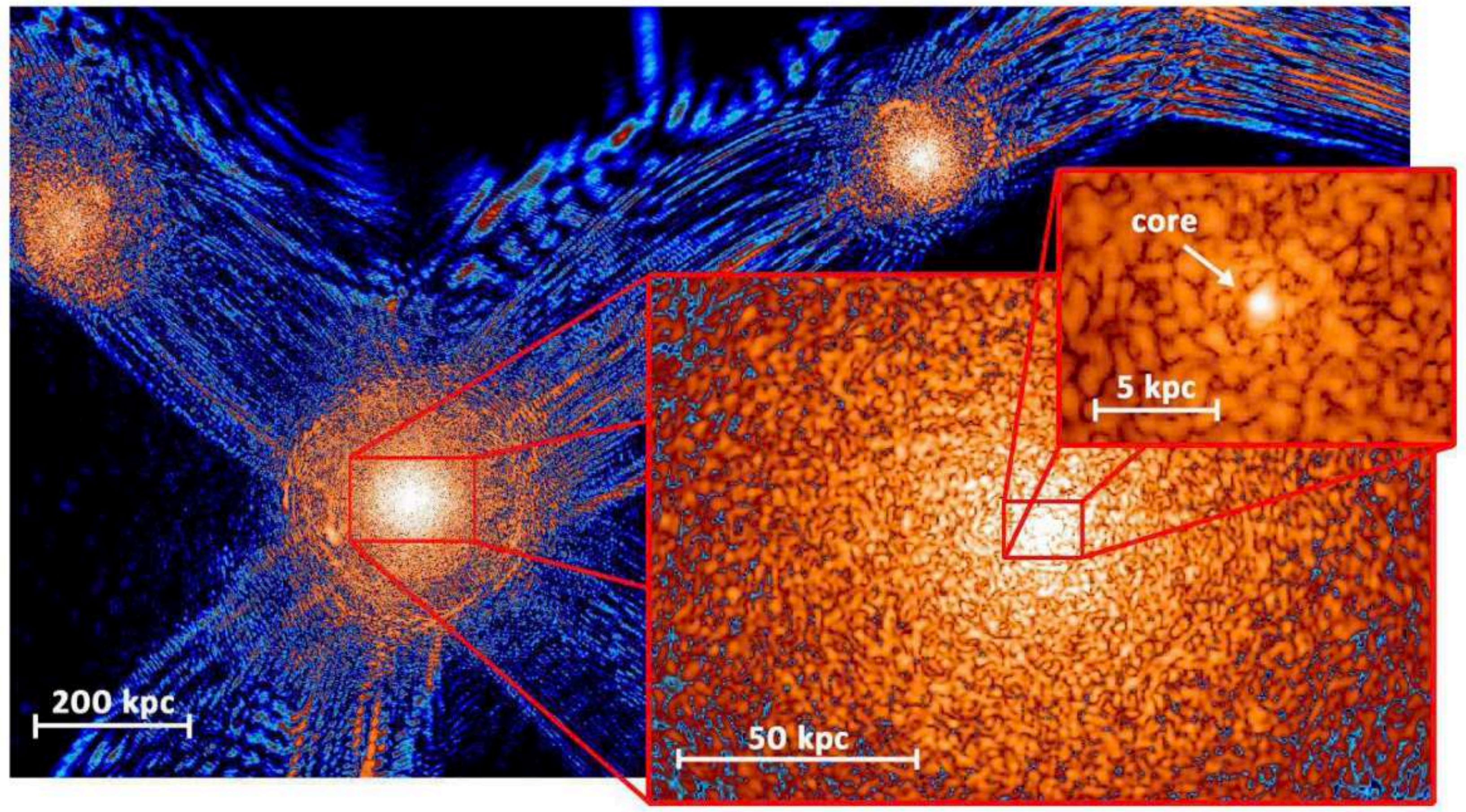

A slice of density field of ψDM simulation on various scales at z=0.1

Schive, Chiueh, and Broadhurst (2014)

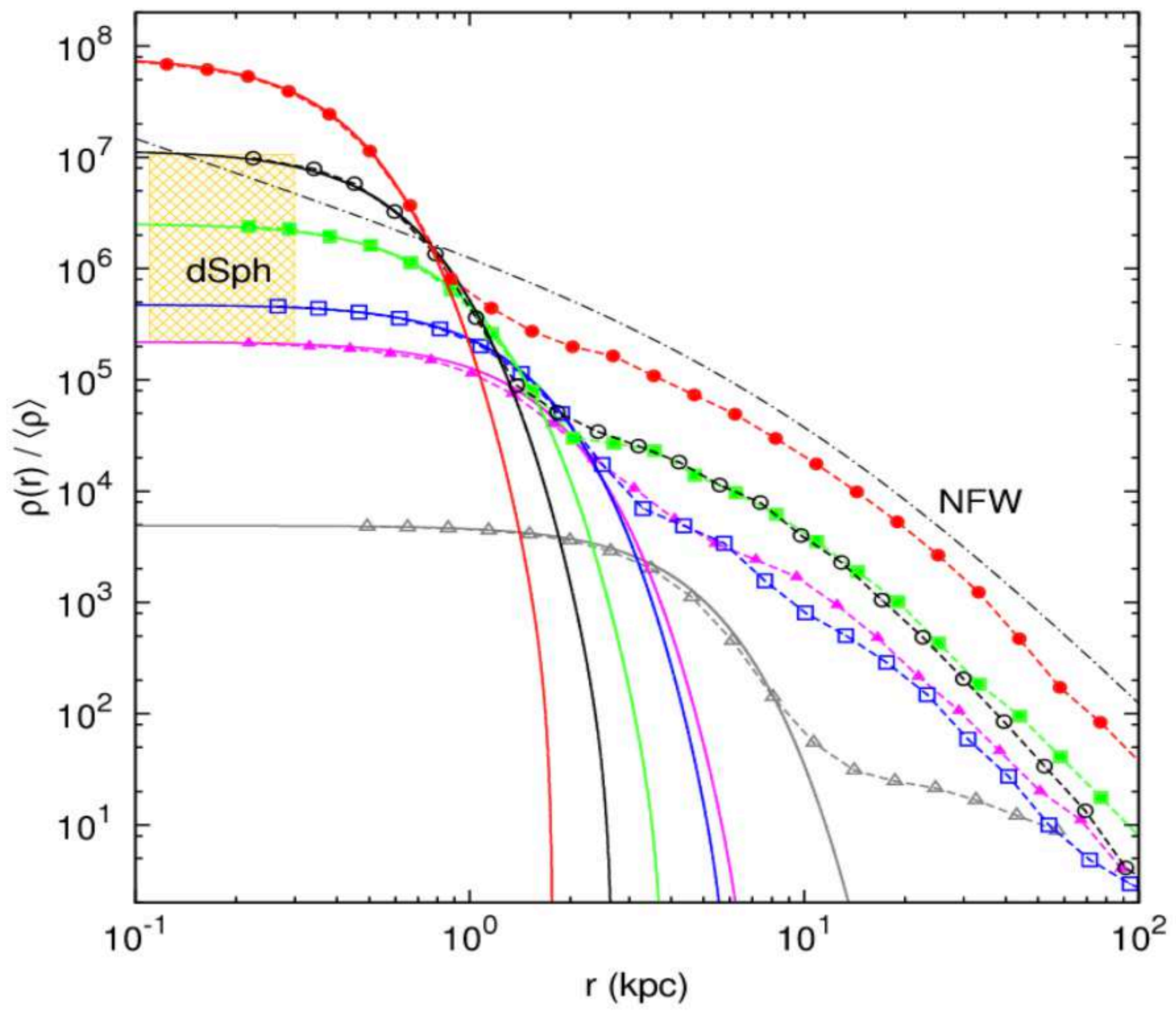

Radial density profiles of haloes formed in the ψDM model

E) Self-interactions

Instead of relying on the quantum pressure (large λ_{dB}), we can also suppress small-scale structures through self-interactions.

This also generates an effective pressure, which is now due to the self-interactions.

II- Fast oscillations in Ultra-light Dark Matter density

A) Background at leading order

$$S_\phi = \int d^4x\sqrt{-g}\left[-\frac{1}{2}g^{\mu\nu}\partial_\mu\phi\partial_\nu\phi - V(\phi)\right].$$

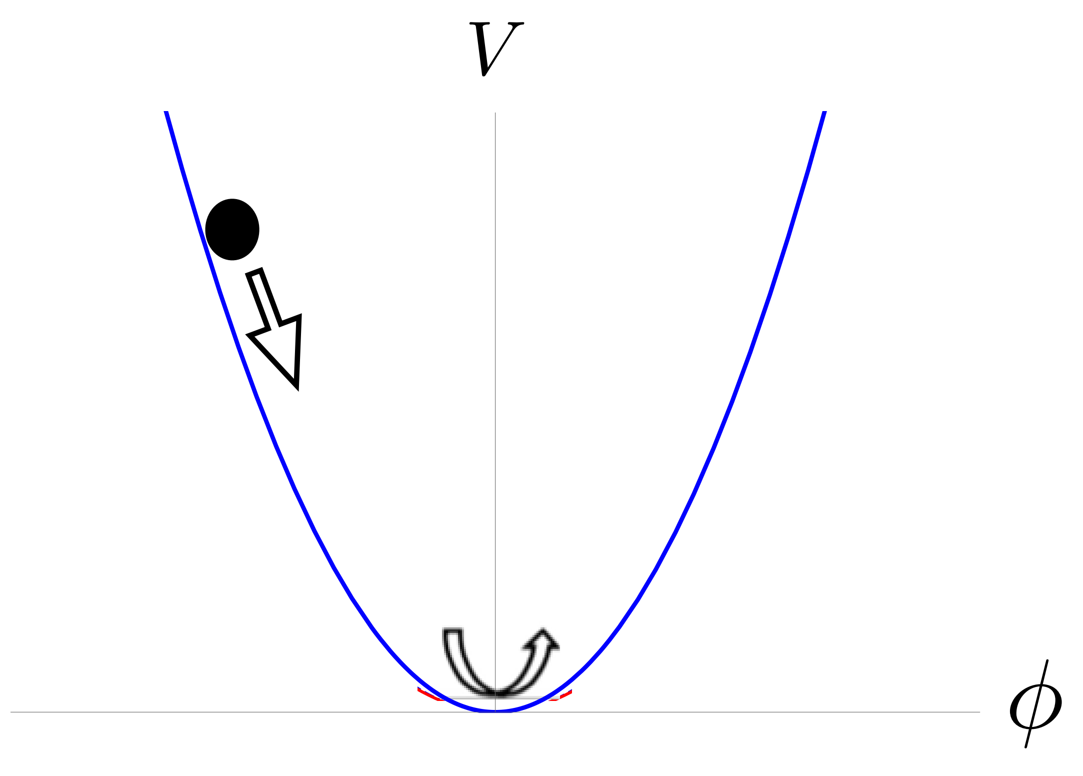

Klein-Gordon . eq.: $\ddot{\phi} + 3H\dot{\phi} + \dfrac{dV}{d\phi} = 0$ e.g., no self-interactions: $V = \dfrac{1}{2}m^2\phi^2$

$H \ll m$ the scalar field oscillates with frequency *m,* and a slow decay of the amplitude:

$$\phi = \phi_0(a/a_0)^{-3/2}\,\cos(mt)$$

$\rho \propto a^{-3}$ → behaves like dark matter:

$V \propto \phi^n$ → $w = \dfrac{\langle p_\phi\rangle}{\langle \rho_\phi\rangle} = \dfrac{n-2}{n+2}$

→ For a mostly quadratic potential with small self-interactions: $V(\phi) = \dfrac{1}{2}m^2\phi^2 + V_{\rm I}(\phi)$ $V_{\rm I} \ll \dfrac{1}{2}m^2\phi^2$

Also, k-essence models: $S_\phi = \displaystyle\int d^4x\sqrt{-g}\left[\Lambda^4 K(X) - \frac{m^2}{2}\phi^2\right]$ $X = -\dfrac{1}{2\Lambda^4}g^{\mu\nu}\partial_\mu\phi\partial_\nu\phi$ $K(X) = X + K_{\rm I}(X)$

$\bar{\phi}(t) = \bar{\varphi}(t)\cos(mt - \bar{S}(t))$ $\bar{\varphi} = \bar{\varphi}_0 a^{-3/2}$ $\bar{S}(t) = \bar{S}_0 - \displaystyle\int_{t_0}^{t} dtm\Phi_{\rm I}\left(\frac{m^2\bar{\varphi}_0^2}{2a^3}\right)$

B) Non-relativistic regime

On the scale of the galactic halo we are in the nonrelativistic regime: the frequencies and wave numbers of interest are much smaller than m and the metric fluctuations are small.

1) From Klein-Gordon eq. to Schrödinger eq.:

Decompose the real scalar field ϕ in terms of the complex scalar field ψ

$$\phi = \frac{1}{\sqrt{2m}}\left(e^{-imt}\psi + e^{imt}\psi^{\star}\right)$$

factorizes (removes) the fast oscillations of frequency m $\qquad \dot{\psi} \ll m\psi, \quad \nabla\psi \ll m\psi$

$\psi(x,t)$ evolves slowly, on astrophysical or cosmological scales.

Instead of the Klein-Gordon eq., it obeys a (non-linear) Schrödinger eq.:

$$\boxed{i\left(\dot{\psi} + \frac{3}{2}H\psi\right) = -\frac{\nabla^2\psi}{2ma^2} + m\Phi_{\rm N}\psi + \frac{\partial\mathcal{V}_{\rm I}}{\partial\psi^{\star}}}$$

Newtonian gravitational potential

self-interactions

$$V_{\rm I}(\phi) = \Lambda^4 \sum_{p\geq 3} \frac{\lambda_p}{p}\left(\frac{\phi}{\Lambda}\right)^p$$

$$\Downarrow$$

$$\mathcal{V}_{\rm I}(\psi,\psi^{\star}) = \Lambda^4 \sum_{p\geq 2} \frac{\lambda_{2p}}{2p}\frac{(2p)!}{(p!)^2}\left(\frac{\psi\psi^{\star}}{2m\Lambda^2}\right)^p$$

(keep only even terms)

2) From Schrödinger eq. to hydrodynamics (Madelung transformation)

Madelung 1927, Chavanis 2012, ...

One can map the Schrödinger eq. to hydrodynamical eqs.: $\psi = \sqrt{\frac{\rho}{m}} e^{is}$ $\vec{v} = \frac{\nabla s}{m}$

The real and imaginary parts of the Schrödinger eq. lead to the continuity and Euler eqs.:

$$\boxed{\dot{\rho} + \nabla \cdot (\rho \vec{v}) = 0}$$

conservation of probability for ψ ➡ conservation of matter for ρ

$$\boxed{\dot{\vec{v}} + (\vec{v} \cdot \nabla)\vec{v} = -\nabla(\Phi_{\rm Q} + \Phi_{\rm N} + \Phi_{\rm I})}$$

Self-interactions

$$\Phi_{\rm I} = \frac{\rho}{\rho_a}$$

effective pressure $P_{\rm eff} \propto \rho^2$

$\gamma = 2$

« quantum pressure » $\Phi_{\rm Q} = -\frac{\nabla^2 \sqrt{\rho}}{2m^2 \sqrt{\rho}}$

comes from part of the kinetic terms in ψ

3) Soliton (ground state): hydrostatic equilibrium

As compared with CDM, the self-interactions allow the formation of hydrostatic equilibrium solutions, with a balance between gravity and the effective pressure:

$$\cancel{\dot{\vec{v}}} + (\vec{v} \cdot \cancel{\nabla})\vec{v} = -\nabla(\cancel{\Phi_{\rm Q}} + \Phi_{\rm N} + \Phi_{\rm I}) \rightarrow \nabla(\Phi_{\rm N} + \Phi_{\rm I}) = 0 \rightarrow \boxed{\rho(r) = \rho_0 \frac{\sin(r/r_a)}{(r/r_a)}}$$

$$R_{\rm sol} \simeq \pi r_a$$

$$\rho_a = \frac{4m^4}{3\lambda_4}, \quad r_a = \frac{1}{\sqrt{4\pi\mathcal{G}\rho_a}}$$

Finite-size halo, called « soliton » or « boson star »

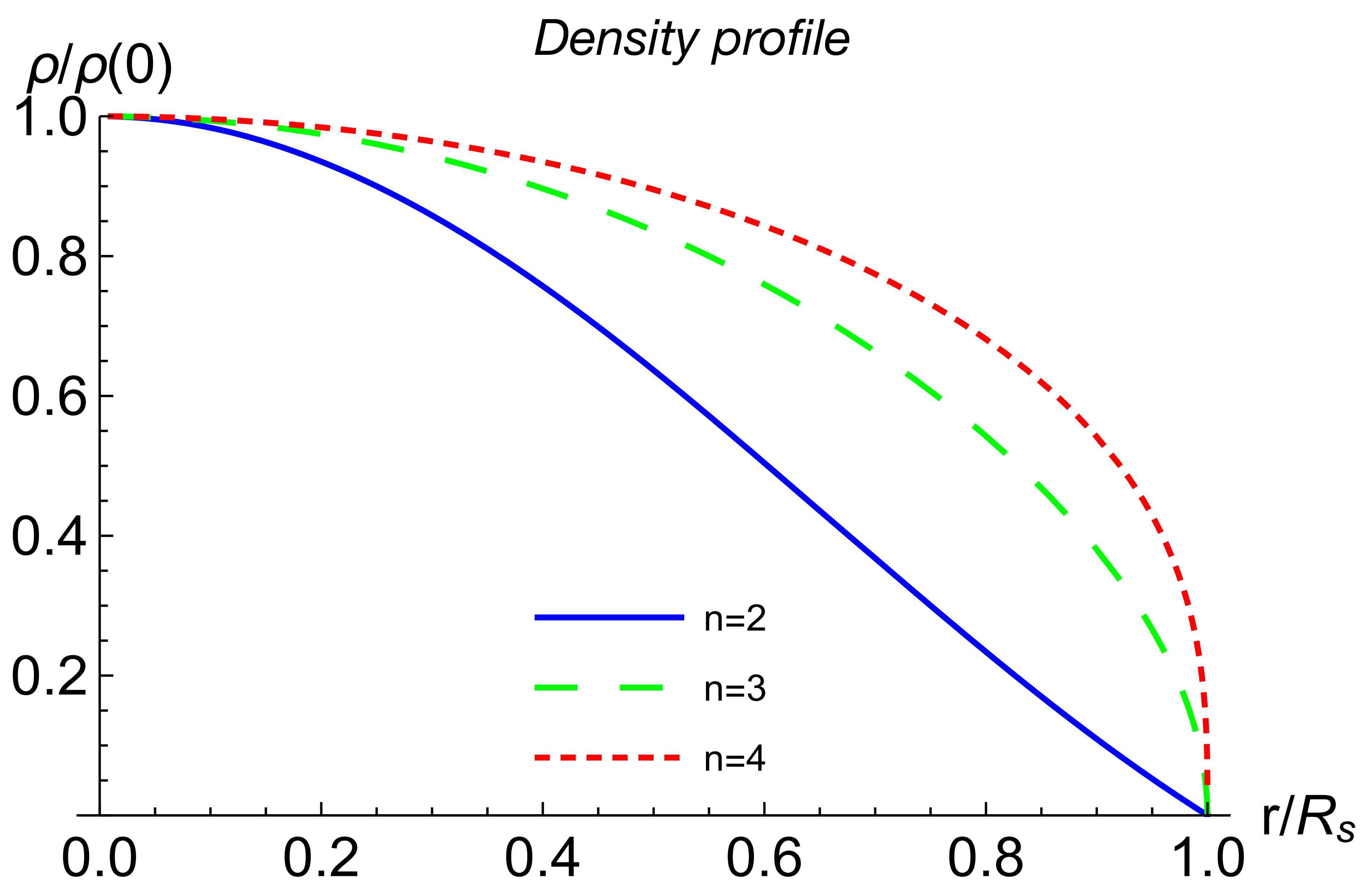

$$V_{\rm I}(\phi) = \Lambda^4 \frac{\lambda_{2n}}{2n} \frac{\phi^{2n}}{\Lambda^{2n}}$$

P. Brax, J. Cembranos, PV, 1906.00730

Ruffini and Bonazolla 1969,
Chavanis 2011,
Schiappacasse and Hertzberg 2018, ...

$m \gg 10^{-18}\mathrm{eV}$: galactic soliton governed by the balance between the repulsive self-interaction and self-gravity.

$m \sim 10^{-21}\mathrm{eV}$: Fuzzy Dark Matter (de Broglie wavelength of galactic size): galactic soliton governed by the balance between the quantum pressure and self-gravity.

Numerical simulations of FDM indeed find that solitons form, from gravitational collapse, within an extended NFW-like out-of-equilibrium halo.

Chen et al. 2020

Schive et al. 2014,
Veltmaat et al. 2018,
Mocz et al. 2019,
Amin and Mocz 2019, ...

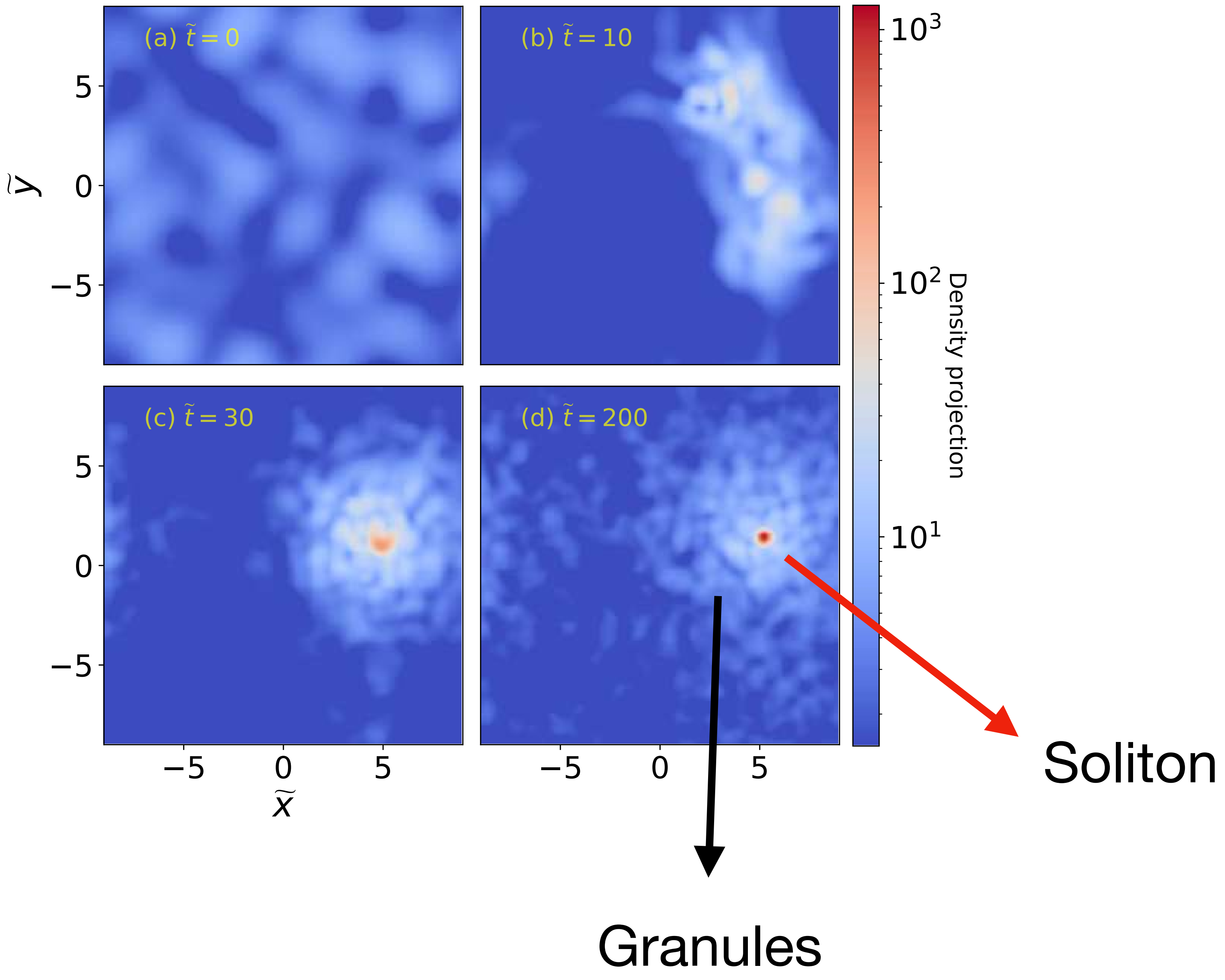

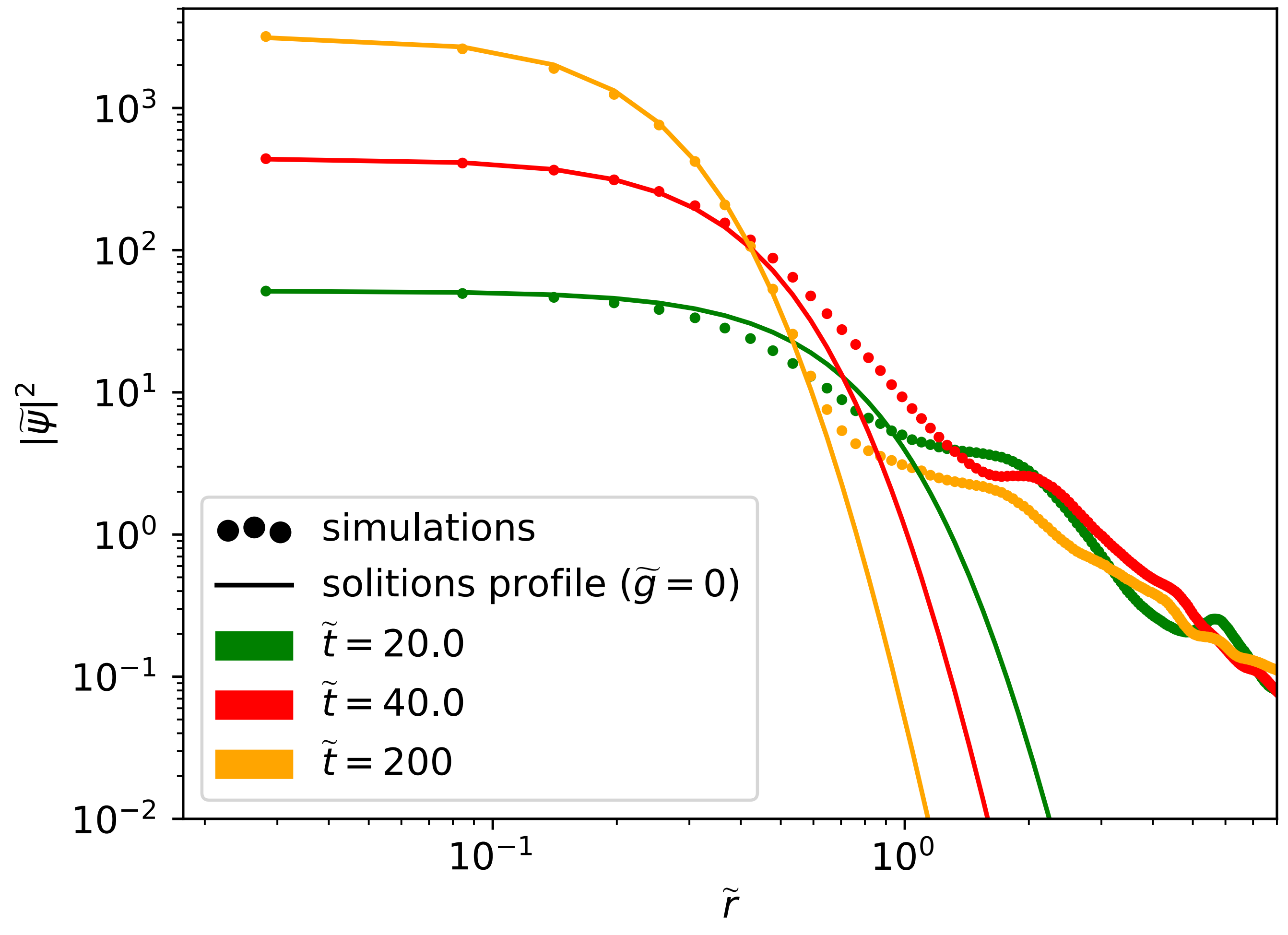

III- Impact of the oscillatory DM gravitational potential on GW

A) DM oscillations

Khmelnitsky & Rubakov. 2013
(shift of PTA time delays)

Brax et al. 2402.04819

Blas et al. 2410.07330

fast oscillations

$$\phi(\vec{x},t) = A(\vec{x},t)\cos[mt + \alpha(\vec{x},t)]$$

slow variations on astrophysical scales

The density field has a subleading oscillatory component: $\rho_{DM} = \rho_0 + \rho_{\rm osc}$

$$T_{\mu\nu} = \partial_\mu\phi\,\partial_\nu\phi - \frac{1}{2}g_{\mu\nu}\left((\partial\phi)^2 - m^2\phi^2\right)$$

$$\rho_0 = \frac{1}{2}m^2A^2 \qquad \rho_{\rm osc} \sim (\nabla\phi)^2 \sim k^2\phi^2 \sim \frac{k^2}{m^2}\rho_0 < v^2\rho_0 \qquad \lambda_{\rm dB} = \frac{2\pi}{mv}, \quad k < \frac{2\pi}{\lambda_{\rm dB}}$$

The gravitational potential also has a subleading oscillatory component:

$$\Psi_N(\vec{x},t) = \Psi_0(\vec{x}) + \Psi_{\rm osc}(\vec{x})\cos[\omega t + 2\alpha(\vec{x})]$$

$$\omega = 2m$$

$$\nabla^2\Psi_0 = 4\pi\mathcal{G}\rho_0 \qquad \Psi_{\rm osc} = \pi\frac{\mathcal{G}\rho}{m^2}$$

B) Frequency shift

In the optical approximation, as for the Sachs-Wolfe effect for CMB photons, the gravitational potential along the line of sight leads to a frequency shift of the GW signal:

$$\frac{\Delta f}{f} = \Psi_N(\vec{x}_e, t_e) - \Psi_N(\vec{x}, t)$$

emission   reception (negligible)

$$f \gtrsim \omega \qquad \text{whence } m_\phi < \left(\frac{f_{\min}}{1 \text{ Hz}}\right) 3 \times 10^{-16} \text{ eV}$$

The integrated Sachs-Wolfe effect is neglected (many oscillations along the l.o.s.): $\lambda = \frac{c}{f} \ll \frac{2\pi}{k}$

This effect is due to the propagation of the GW from the source to the observer, not to new physics modifying the production of the GW.

C) GW phase shift

GW signal: $h(t) = A(t)\cos[\Phi(t)]$

Phase and time related to the frequency drift: $\Phi = 2\pi \int df \frac{f}{\dot{f}}, \qquad t = \int df \frac{1}{\dot{f}}$

Going to Fourier space: $$\tilde{h}(f) = \int dt\, e^{i2\pi f t} h(t) = A(f) e^{i\psi(f)}$$

Saddle-point approximation: $A(f) \propto f^{-7/6}, \qquad \psi(f) = 2\pi f t_\star - \Phi(t_\star) - \pi/4, \qquad f(t_\star) = f.$

At leading order, the frequency drift is due to the emission of GW:

$$\bar{\psi}(f) = 2\pi f t_c - \Phi_c - \frac{\pi}{4} + \psi_{\rm GW}(f),$$

$$\psi_{\rm GW}(f) = \frac{3}{128}\left(\frac{\pi \mathcal{G}\mathcal{M} f}{c^3}\right)^{-5/3}\left[1 + \left(\frac{3715}{756} + \frac{55\nu}{9}\right)\left(\frac{\pi \mathcal{G} M f}{c^3}\right)^{2/3}\right]$$

$$M = m_1 + m_2, \quad \nu = m_1 m_2 / M^2, \quad \mathcal{M} = \nu^{3/5} M$$

The Sachs-Wolfe effect due to the DM gravitational potential gives a contribution (due to the correction to the observed frequency):

$$\Delta\psi(f) = 2\pi \int_{\bar{t}_\star}^{t_c} dt \bar{f} \Psi.$$

The contribution from the constant part is degenerate with the leading GW contribution:

$$\Delta\psi_0(f) = \frac{\Psi_0}{16}\left(\frac{\pi \mathcal{G}\mathcal{M} f}{c^3}\right)^{-5/3}$$

incomplete Gamma function

The contribution from the oscillatory part reads:

$$\Delta\psi_{\rm osc}(f) = \Psi_{\rm osc} 2\pi \left(\frac{5}{256\pi}\right)^{3/8}\left(\frac{\pi \mathcal{G}\mathcal{M}\omega}{c^3}\right)^{-5/8} {\rm Re}[e^{i(5\pi/16 + \theta - \omega t_c)}\gamma(5/8, -iy)]$$

$$y = \omega(t_c - \bar{t}_\star) = \frac{m_\phi}{m_\star}, \quad m_\star = f\,\frac{128\pi}{5}\left(\frac{\pi \mathcal{G}\mathcal{M} f}{c^3}\right)^{5/3}$$

Low scalar mass, degeneracy with leading GW term

$$m_\phi \ll m_\star: \; \Delta\psi_{\rm osc}(f) = \frac{\Psi_{\rm osc}}{16}\left(\frac{\pi \mathcal{G}\mathcal{M} f}{c^3}\right)^{-5/3}\cos(\omega t_c - \theta)$$

Large scalar mass, degeneracy with constant factor Φ_c

$$m_\phi \gg m_\star: \; \Delta\psi_{\rm osc}(f) = \Psi_{\rm osc}\Gamma(5/8) 2\pi \left(\frac{5}{256\pi}\right)^{3/8}\left(\frac{\pi \mathcal{G}\mathcal{M}\omega}{c^3}\right)^{-5/8}\cos(\omega t_c - \theta - 5\pi/16)$$

Probe scalar masses $m \sim m_\star,$ $m_\star \ll f$ for $(\mathcal{G}\mathcal{M} f / c^3) \ll 1, \quad R_{\rm Sch} \ll \lambda$

D) Comparison with dynamical friction

In many cases (CDM, supersonic motion in fluids or SFDM), the drag force on a BH moving within a medium takes the form of the Chandrasekhar result:

$$m_i \dot{\vec{v}}_i = -\frac{4\pi\mathcal{G}^2 m_i^2 \rho}{v_i^3} \Lambda \vec{v}_i,$$

This gives a correction to the frequency drift and to the GW phase, which is independent of the scalar mass:

$$\Delta\psi_{\rm df} = -\frac{75}{38912} \frac{\pi\mathcal{G}^3\mathcal{M}\rho}{c^6} \left(\frac{\pi\mathcal{G}\mathcal{M}f}{c^3}\right)^{-16/3} \frac{\Lambda(m_1^3+m_2^3)}{\nu^{1/5}\mathcal{M}^3}$$

E) Fisher matrix analysis

	m_1 ($M_\odot$)	m_2 ($M_\odot$)	SNR	d_L (Mpc)	detections
MBBH	10^6	5×10^5	3×10^4	10^3	0.4 - 600
IBBH	10^4	5×10^3	708	10^3	0.4 - 600
IMRI	10^4	10	64	10^3	8 - 80
EMRI	10^5	10	22	10^3	20 - 400
WD	0.4	0.3	7	5×10^{-3}	10^4

$$\Gamma_{ij} = \frac{(\mathrm{SNR})^2}{\int_{f_{\rm min}}^{f_{\rm max}} \frac{df}{S_n(f)} f^{-7/3}} \int_{f_{\rm min}}^{f_{\rm max}} \frac{df}{S_n(f)} f^{-7/3} \frac{\partial\psi}{\partial\theta_i}\frac{\partial\psi}{\partial\theta_j}$$

$$\{\theta_i\} = \{t_c, \Phi_c, \ln(m_1), \ln(m_2), \Psi_{\rm osc}\}$$

F) LISA

Detection thresholds for 1 event (comparison of various binary systems)

DM gravitational potential

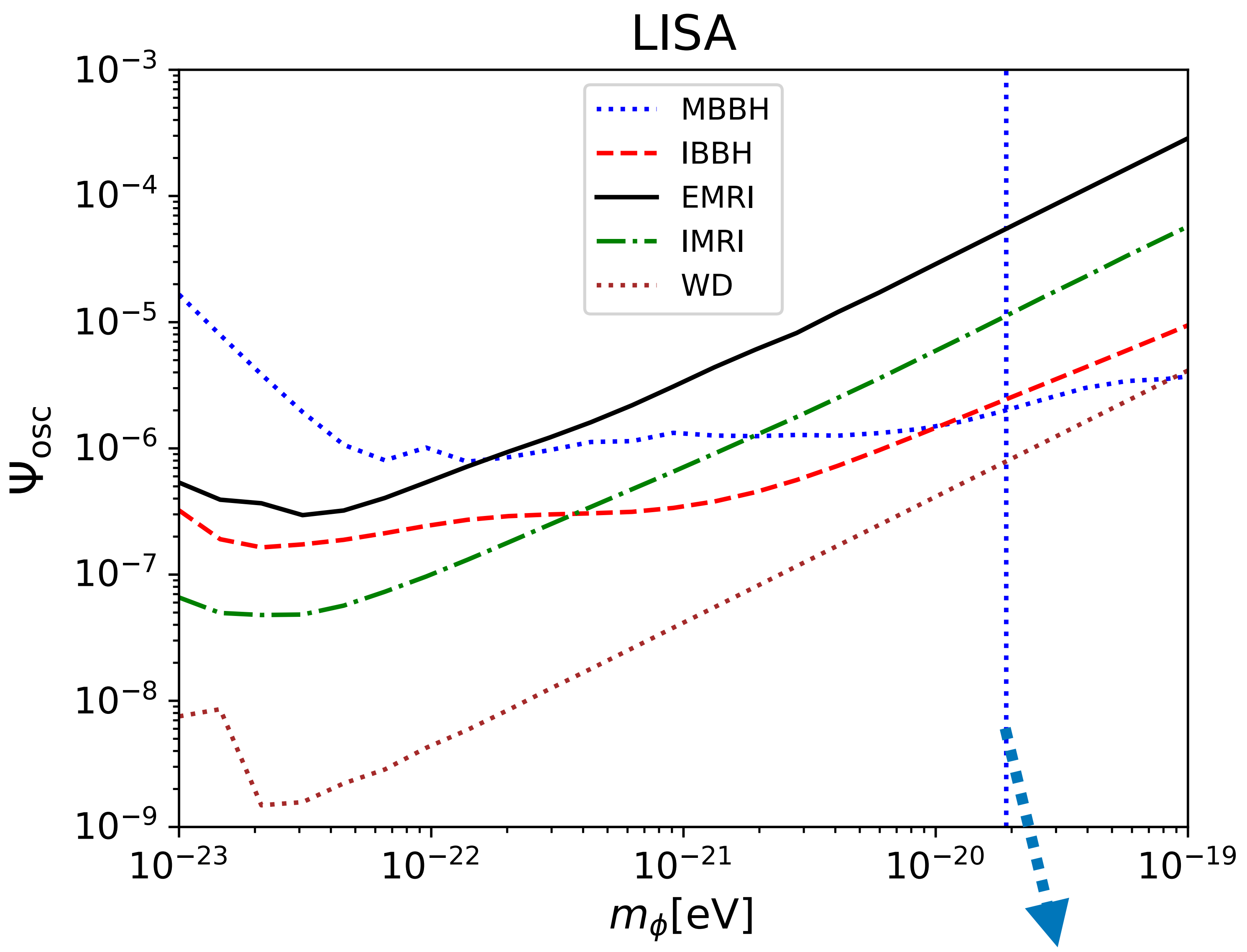

$2m < f_{\rm min}$ for MBBH

DM density

relativistic DM cloud

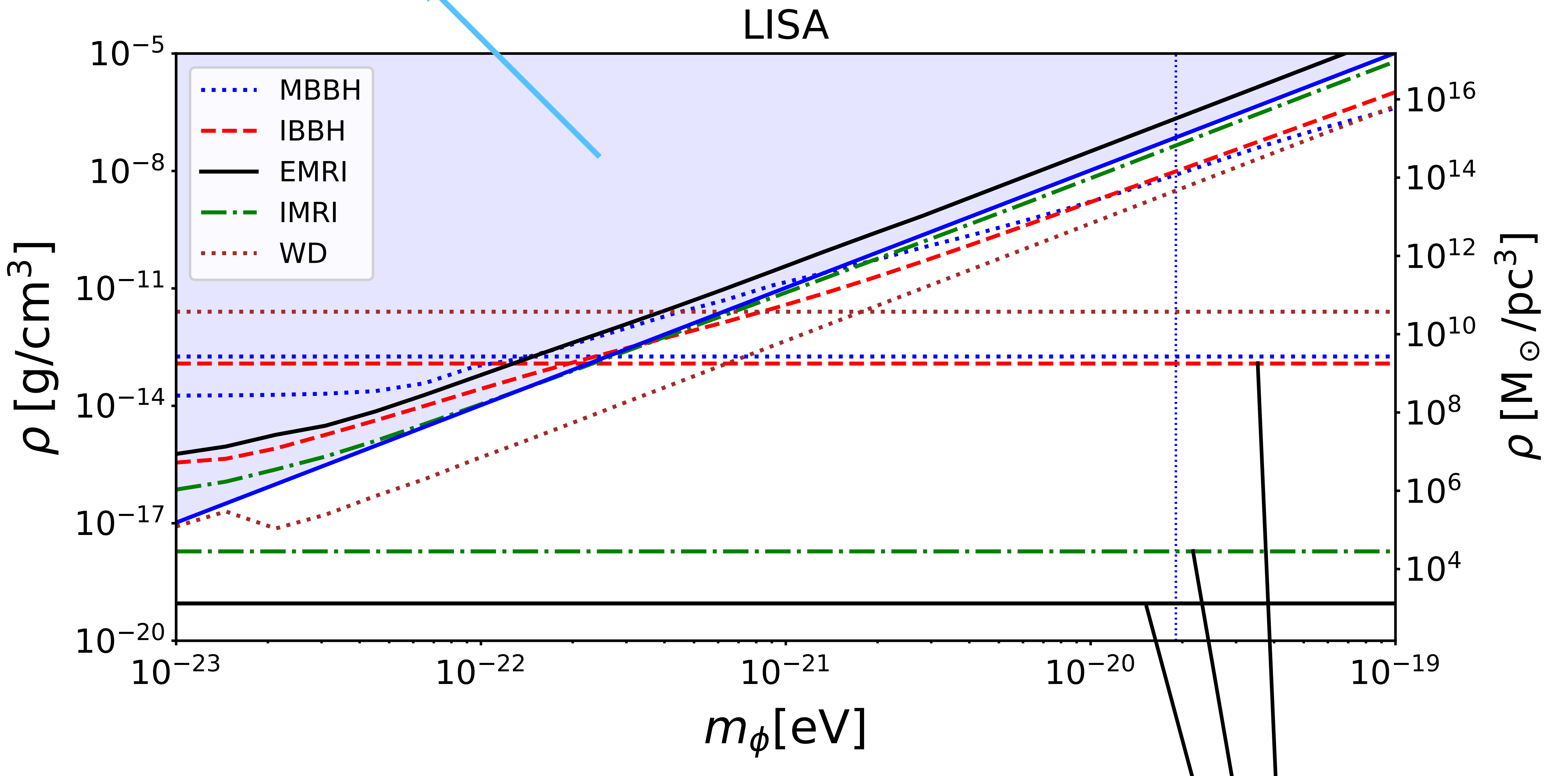

dynamical friction

$$\Delta\psi_{\rm osc}(f) \sim \Psi_{\rm osc} 2\pi \left(\frac{5}{256\pi}\right)^{3/8} \left(\frac{\pi\mathcal{G}\mathcal{M}2m_\phi}{c^3}\right)^{-5/8} \left|\gamma\left(\frac{5}{8}, -i\frac{m_\phi}{m_\star(f)}\right)\right|$$

$$\Psi_{\rm osc} = \pi\frac{\mathcal{G}\rho}{m_\phi^2} \qquad \sigma_\rho \propto m^2 \sigma_{\Psi_{\rm osc}}$$

WD have smaller mass, which improves the detection threshold.

The density threshold increases with the scalar mass.

For $m_\phi \gtrsim 10^{-21}$ eV dynamical friction is more important than the oscillations of the DM potential.

Non-relativistic DM cloud: $\rho = \frac{M_{\rm cloud}}{R^3} < \frac{M_{\rm cloud}}{\lambda_c^3} = \frac{M_{\rm cloud}}{1 M_\odot}\left(\frac{m_\phi}{1 \text{ eV}}\right)^3 10^{45} \text{ g/cm}^3$

$\lambda_C = \frac{2\pi}{m_\phi} = \left(\frac{m_\phi}{1 \text{ eV}}\right)^{-1} 4\times 10^{-23}$ pc. Compton wavelength

G) DECIGO

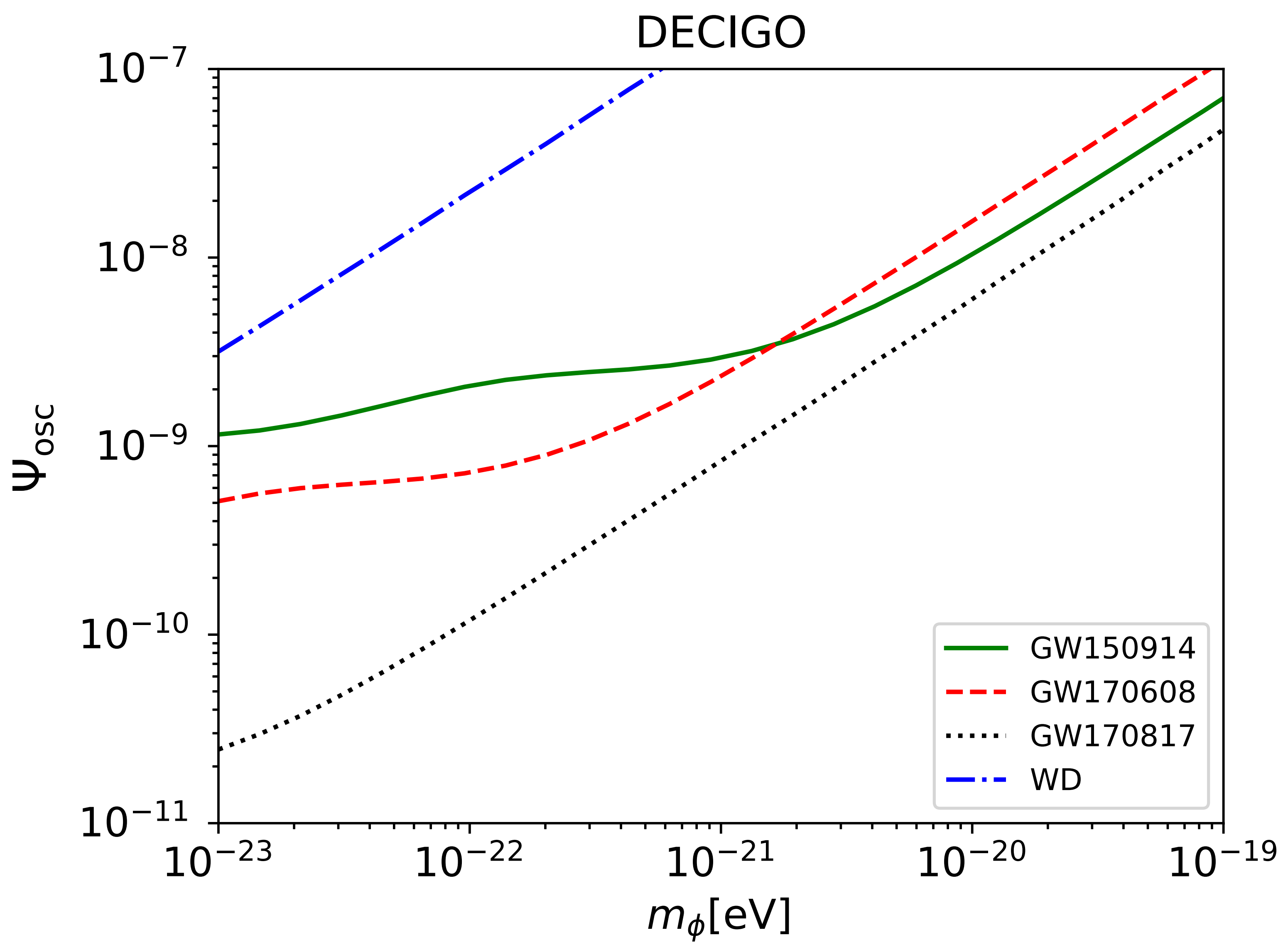

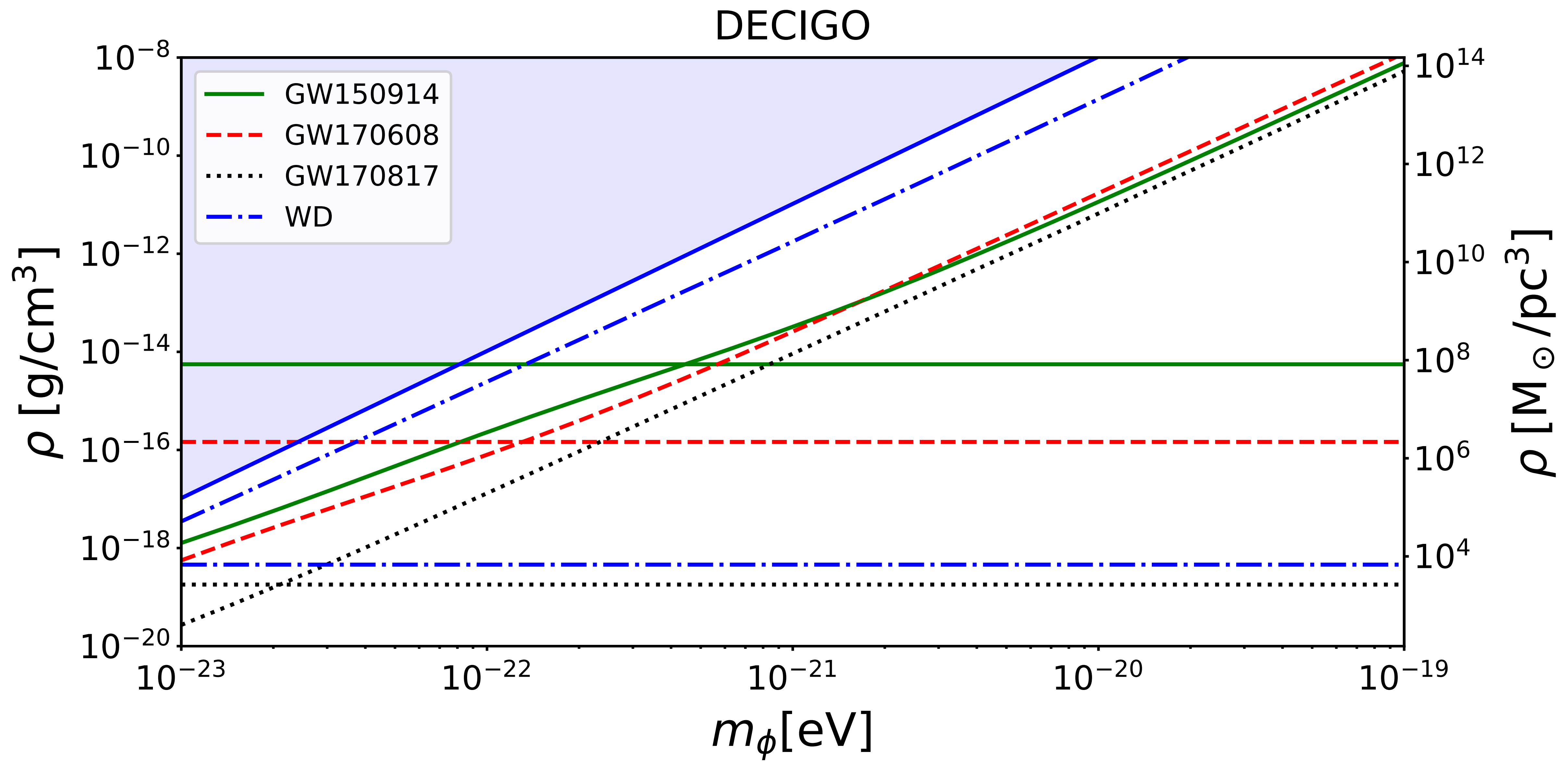

The detection thresholds are of the same order as for LISA, but somewhat better.

IV- Conclusion

This probe is unlikely to be competitive with other more direct observations of DM substructures.

For $m_\phi > 10^{-21}$ eV standard effects such as dynamical friction (accretion, gravitational pull) are expected to dominate.

For $m_\phi < 10^{-23}$ eV the clouds that could be detected would have a Compton wavelength greater than 1 pc.

For $m_\phi \sim 10^{-22}$ eV the clouds that could be detected by LISA would have a density that is greater than in the solar neighbourhood by a factor of 10^5, a mass above $10^5\, M_\odot$ and a radius above $0.4\,\mathrm{pc}$

non-standard formation mechanism at $z \sim 10^4$

→ Except for a small region of the DM parameter space, standard analysis where such an effect is neglected are justified.

Gravitational Waves emitted by a BH binary inside a SFDM soliton

Collaboration with A. Boudon, Ph. Brax

Boudon et al. 2305.18540

I- Additional forces on the BHs due to the dark matter environment

Gravity of the dark matter cloud:

$$m_{\mathrm{BH}}\dot{\mathbf{v}}_{\mathrm{BH}}|_{\mathrm{halo}} = -\frac{4\pi}{3}\mathcal{G}m_{\mathrm{BH}}\rho_0(\mathbf{x}-\mathbf{x}_0)$$

Accretion drag:

$$m_{\mathrm{BH}}\dot{\mathbf{v}}_{\mathrm{BH}}|_{\mathrm{acc}} = -\dot{m}_{\mathrm{BH}}\mathbf{v}_{\mathrm{BH}}$$

Dynamical friction:

$$m_{\mathrm{BH}}\dot{\mathbf{v}}_{\mathrm{BH}}|_{\mathrm{df}} = -\frac{8\pi\mathcal{G}^2 m_{\mathrm{BH}}^2\rho_0}{3v_{\mathrm{BH}}^3}\ln\left(\frac{r_{\mathrm{IR}}}{r_{\mathrm{UV}}}\right)\mathbf{v}_{\mathrm{BH}}$$

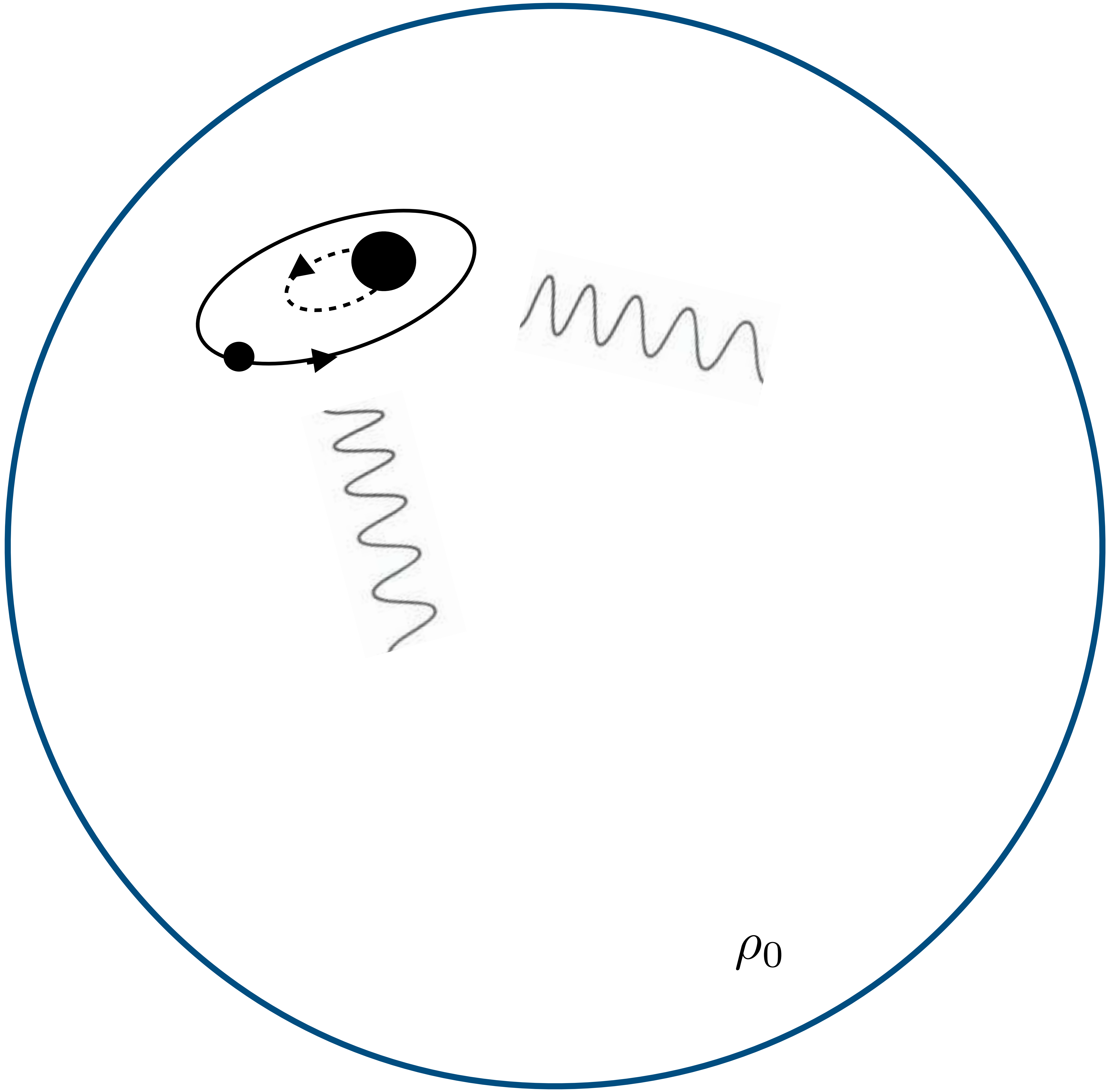

II- Decay of the orbital radius

$$\langle \dot{a} \rangle = \langle \dot{a} \rangle_{\rm acc} + \langle \dot{a} \rangle_{\rm df} + \langle \dot{a} \rangle_{\rm gw}$$

$$\langle \dot{a} \rangle_{\rm gw} = -\frac{64\nu \mathcal{G}^3 m^3}{5c^5 a^3}\left(1 - \frac{4\pi\rho_0 a^3}{3m}\right)$$

Correction due to the halo bulk gravity

$$\langle \dot{a} \rangle_{\rm acc} = -a A_{\rm acc} - a\left(\frac{a}{\mathcal{G}m}\right)^{3/2} B_{\rm acc}$$

Accretion drag

$$\langle \dot{a} \rangle_{\rm df} = -a\left(\frac{a}{\mathcal{G}m}\right)^{3/2}\left[B_{\rm df} + C_{\rm df}\ln\left(\sqrt{\frac{\mathcal{G}m}{a}}\frac{1}{c_s}\right)\right]$$

Dynamical friction

III- Phase of the GW waveform

GW frequency: $$\mathfrak{f} = \frac{1}{\pi}\sqrt{\frac{\mathcal{G}m}{a^3}}\left(1 + \frac{2\pi\rho_0 a^3}{3m}\right)$$

Frequency drift: $$\dot{\mathfrak{f}} = \frac{1}{\pi}\sqrt{\frac{\mathcal{G}m}{a^3}}\left(\frac{\dot{m}}{2m} - \frac{3\dot{a}}{2a}\right) + \mathcal{G}\rho_0\left(\frac{a^3}{\mathcal{G}m}\right)^{1/2}\frac{\dot{a}}{a}$$

Phase: $\Phi(t) = 2\pi \int d\mathfrak{f}\,(\mathfrak{f}/\dot{\mathfrak{f}})$

Time: $t = \int d\mathfrak{f}\,(1/\dot{\mathfrak{f}})$

Fourier transform of the GW signal: $\boxed{\tilde{h}(f) = \mathcal{A}(f)e^{i\Psi(f)}}$

Phase: $$\boxed{\Psi(f) = 2\pi f t_c - \Phi_c - \frac{\pi}{4} + \Psi_{\rm gw} + \Psi_{\rm halo} + \Psi_{\rm acc} + \Psi_{\rm df}}$$

DM corrections

$$\Psi_{\rm gw} = \frac{3}{128}\left(\frac{\pi\mathcal{G}\mathcal{M}f}{c^3}\right)^{-5/3}\left[1 + \frac{20}{9}\left(\frac{743}{336} + \frac{11}{4}\nu\right)\left(\frac{\pi\mathcal{G}mf}{c^3}\right)^{2/3}\right]$$

O + 1 PN

$\Psi_{\rm halo}$ -3 PN

$\Psi_{\rm acc}$ -4.5 / -5.5 PN

$\Psi_{\rm df}$ -5.5 PN

$$\Psi_{\rm halo} = \frac{25\pi}{924}\frac{\rho_0\mathcal{G}^3\mathcal{M}^2}{c^6}(\pi\mathcal{G}\mathcal{M}f/c^3)^{-11/3}$$

$$\Psi_{\rm acc} = -\frac{25\pi\mathcal{G}^3\mathcal{M}^2\rho_0}{38912c^6}\left(\frac{\pi\mathcal{G}\mathcal{M}f}{c^3}\right)^{-16/3}\sum_{i=1}^{2}\Theta(f > f_{{\rm acc},i})\frac{m_i^3}{\mu^2 m}\left(3+2\frac{m_i^2}{m\mu}\right)$$
$$-\frac{75\pi F_\star\nu^{2/5}\mathcal{G}^3\mathcal{M}^2\rho_a}{26624c^6}\left(\frac{\pi\mathcal{G}\mathcal{M}f}{c^3}\right)^{-13/3}\sum_{i=1}^{2}\Theta(f < f_{{\rm acc},i})\left(3+2\frac{m_i^2}{m\mu}\right)\left[1-\left(\frac{f}{f_{{\rm acc},i}}\right)^{13/3}+\frac{13}{19}\left(\frac{f}{f_{{\rm acc},i}}\right)^{16/3}\right]$$

$$\Psi_{\rm df} = \frac{875\pi\mathcal{G}^3\mathcal{M}^2\rho_0}{11829248c^6}\left(\frac{\pi\mathcal{G}\mathcal{M}f}{c^3}\right)^{-16/3}\sum_{i=1}^{2}\frac{m_i^3}{\mu^2 m}\Theta(f^-_{{\rm df},i}<f^+_{{\rm df},i})\Bigg\{\Theta(f^-_{{\rm df},i}<f<f^+_{{\rm df},i})\left[1+\frac{304}{105}\ln\frac{f}{f^+_{{\rm df},i}}-\frac{361}{105}\left(\frac{f}{f^+_{{\rm df},i}}\right)^{16/3}+\frac{256}{105}\left(\frac{f}{f^+_{{\rm df},i}}\right)^{19/3}\right]$$
$$+\Theta(f<f^-_{{\rm df},i})\left[-\frac{361}{105}\left(\frac{f}{f^+_{{\rm df},i}}\right)^{16/3}+\frac{361}{105}\left(\frac{f}{f^-_{{\rm df},i}}\right)^{16/3}+\frac{5776}{315}\left(\frac{f}{f^-_{{\rm df},i}}\right)^{16/3}\ln\frac{f^-_{{\rm df},i}}{f^+_{{\rm df},i}}+\frac{256}{105}\left(\frac{f}{f^+_{{\rm df},i}}\right)^{19/3}-\frac{256}{105}\left(\frac{f}{f^-_{{\rm df},i}}\right)^{19/3}-\frac{4864}{315}\left(\frac{f}{f^-_{{\rm df},i}}\right)^{19/3}\ln\frac{f^-_{{\rm df},i}}{f^+_{{\rm df},i}}\right]\Bigg\}$$

IV- Fisher matrix analysis

$$\Gamma_{ij} = \frac{(\mathrm{SNR})^2}{\int_{f_{\min}}^{f_{\max}} \frac{df}{S_n(f)} f^{-7/3}} \int_{f_{\min}}^{f_{\max}} \frac{df}{S_n(f)} f^{-7/3} \frac{\partial \Psi}{\partial \theta_i} \frac{\partial \Psi}{\partial \theta_j}$$

Parameters: $\{\theta_i\} = \{t_c, \Phi_c, \ln(m_1), \ln(m_2), \rho_0, \rho_a\}$

ρ_0 halo bulk density

$$\rho_a = \frac{4m^4}{3\lambda_4}$$

V- Region in the parameter space that can be detected

ρ_0 halo bulk density

LISA:

BHL accretion mode

Plane (ρ_0, ρ_a)

$$\rho_a = \frac{4m^4}{3\lambda_4}$$

Max. radial accretion mode

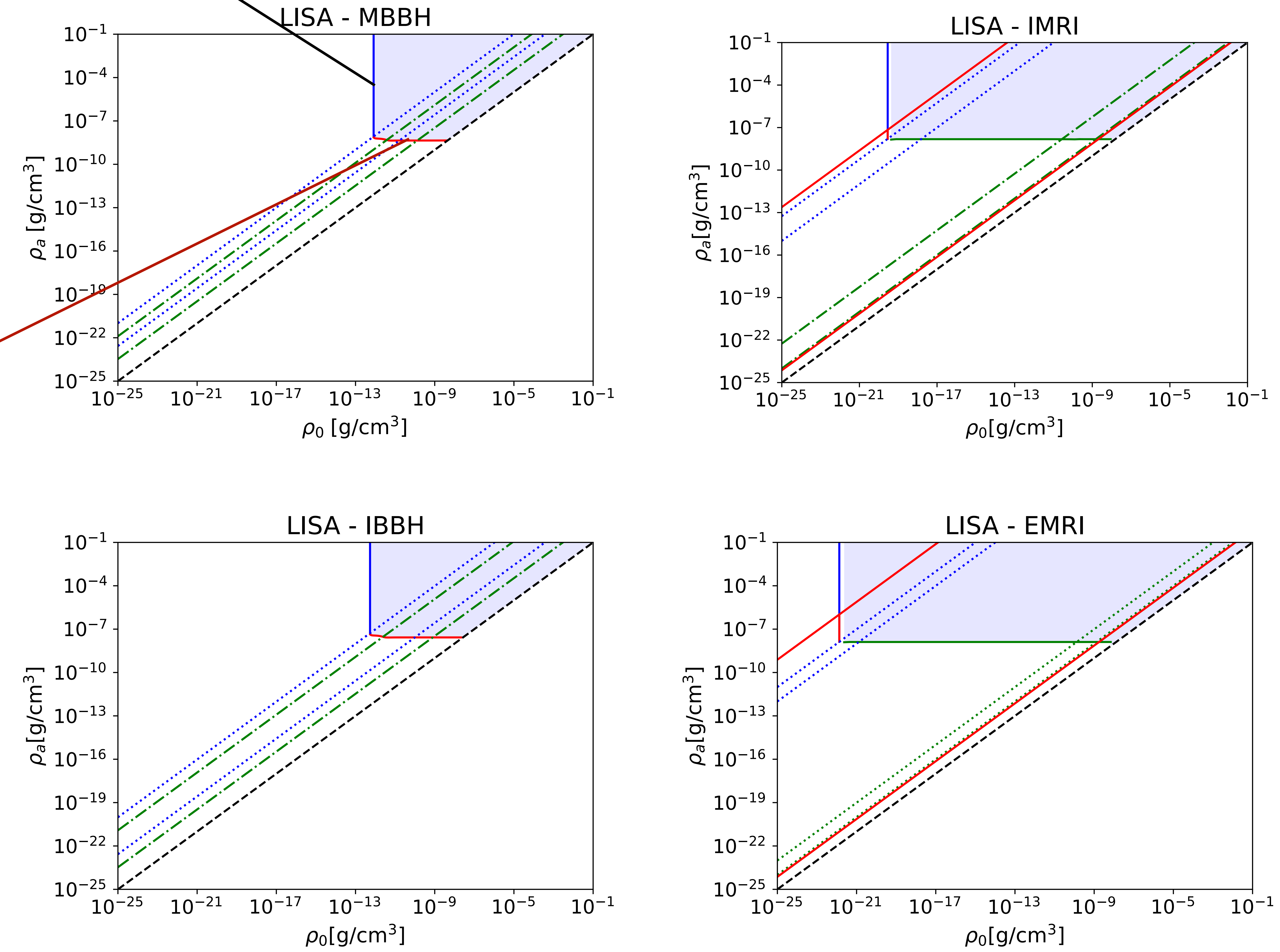

$$\frac{\rho_a}{\rho_0} = \frac{c^2}{c_s^2} \geq 1$$

Event \ Properties	m_1 ($M_\odot$)	m_2 ($M_\odot$)	χ_1	χ_2	$\chi_{\rm eff}$
MBBH	10^6	5×10^5	0.9	0.8	0.87
IBBH	10^4	5×10^3	0.3	0.4	0.33
IMRI	10^4	10	0.8	0.5	0.80
EMRI	10^5	10	0.8	0.5	0.80

$$1\ M_\odot/\mathrm{pc}^3 = 6.7\times10^{-23}\ \mathrm{g/cm}^3$$

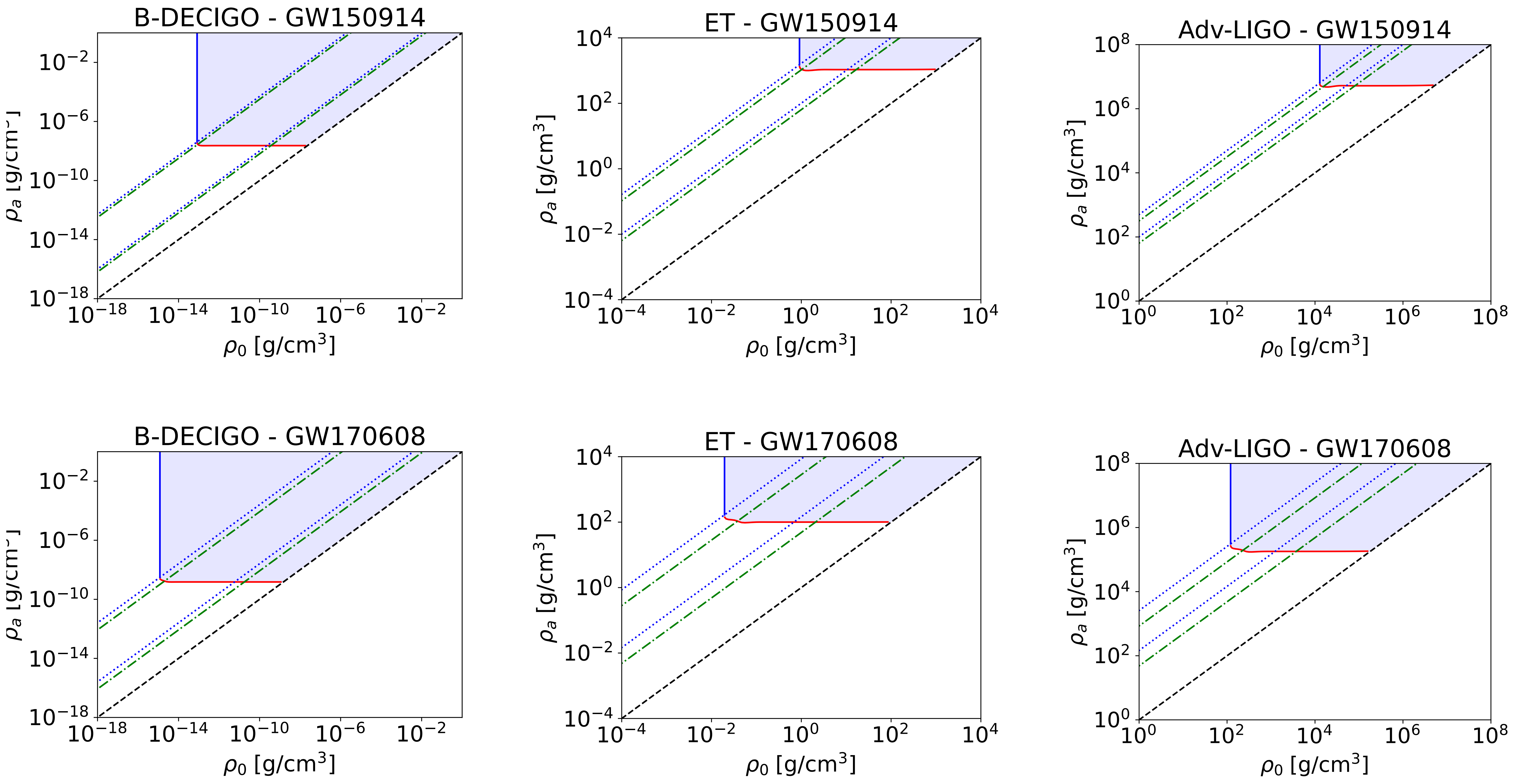

Detector / Event	LISA	B-DECIGO	ET	Adv-LIGO
MBBH	$\rho_0 > 8 \times 10^{-13}$ g/cm^3 $\rho_a > 5 \times 10^{-9}$ g/cm^3	× ×	× ×	× ×
IBBH	$\rho_0 > 5 \times 10^{-13}$ g/cm^3 $\rho_a > 3 \times 10^{-8}$ g/cm^3	× ×	× ×	× ×
IMRI	$\rho_0 > 3 \times 10^{-20}$ g/cm^3 $\rho_a > 2 \times 10^{-8}$ g/cm^3	× ×	× ×	× ×
EMRI	$\rho_0 > 10^{-22}$ g/cm^3 $\rho_a > 10^{-8}$ g/cm^3	× ×	× ×	× ×
GW150914	× ×	$\rho_0 > 8 \times 10^{-14}$ g/cm^3 $\rho_a > 2 \times 10^{-8}$ g/cm^3	$\rho_0 > 0.9$ g/cm^3 $\rho_a > 10^3$ g/cm^3	$\rho_0 > 10^4$ g/cm^3 $\rho_a > 5 \times 10^6$ g/cm^3
GW170608	× ×	$\rho_0 > 10^{-15}$ g/cm^3 $\rho_a > 2 \times 10^{-9}$ g/cm^3	$\rho_0 > 0.02$ g/cm^3 $\rho_a > 101$ g/cm^3	$\rho_0 > 120$ g/cm^3 $\rho_a > 2 \times 10^5$ g/cm^3

ρ_0 halo bulk density

$$\rho_a = \frac{4m^4}{3\lambda_4}$$

Critical density:

$$\rho_c \sim 10^{-29}\mathrm{g/cm^3} \sim 10^{-7} M_\odot/\mathrm{pc}^3$$

Solar neighborhood:

$$\rho_{\rm DM} \sim 1\ M_\odot/\mathrm{pc}^3 \sim 7 \times 10^{-23}\ \mathrm{g/cm^3}$$

Baryonic density in thick disks:

$$\rho_{\rm b} \lesssim 10^{-7}\mathrm{g/cm^3}$$

Plane $(m_{\rm DM}, \lambda_4)$

Models with coupling below this line can be detected

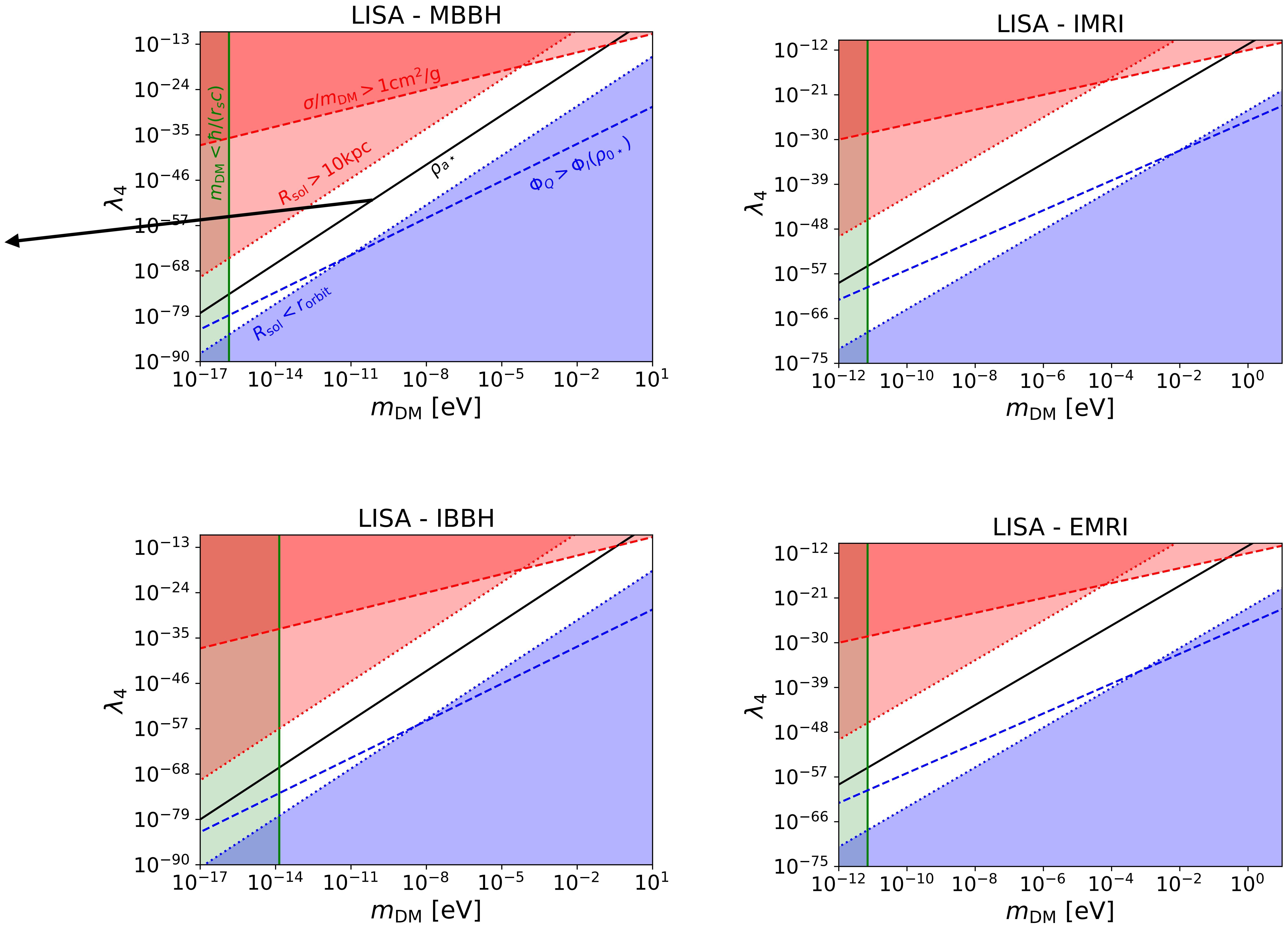

Plane $(m_{\rm DM}, R_{\rm sol})$

$$R_{\rm sol} = \pi\sqrt{\frac{3\lambda_4}{2}\frac{M_{\rm Pl}}{m^2}}$$

$$R_{\rm sol} = \sqrt{\frac{\pi}{4\mathcal{G}\rho_a}}$$

Radius of the scalar cloud (soliton)

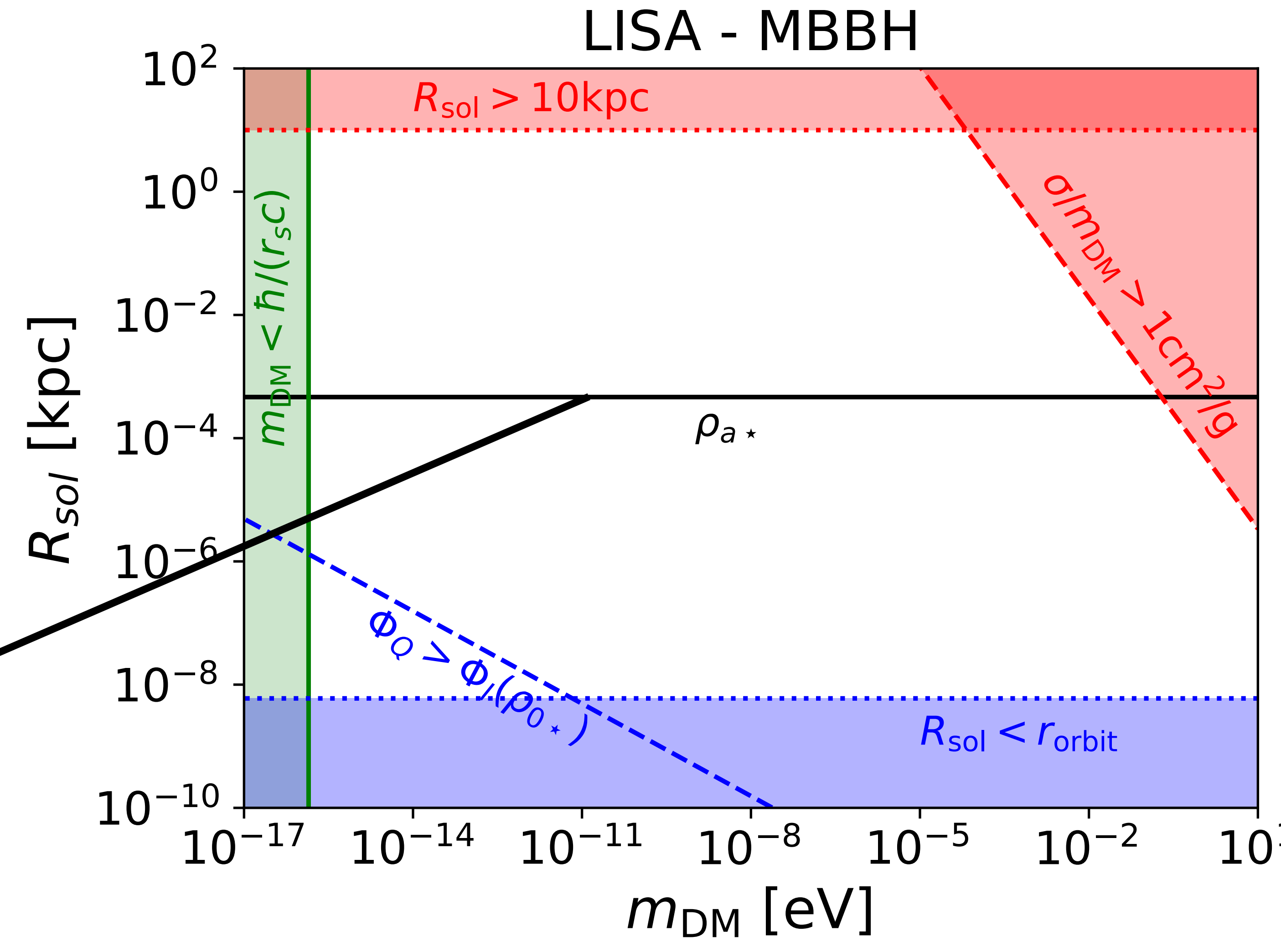

Models with soliton radius below this line can be detected